Neurosci. Bull. December, 2019, 35(6):996–1010
https://doi.org/10.1007/s12264-019-00384-7

www.neurosci.cn
www.springer.com/12264

ORIGINAL ARTICLE

Development of Human *in vitro* Brain-blood Barrier Model from Induced Pluripotent Stem Cell-derived Endothelial Cells to Predict the *in vivo* Permeability of Drugs

Yuan Li[1,2] · Xueying Sun[2] · Houfu Liu[2] · Liang Huang[2] · Guofeng Meng[2] · Yu Ding[3] · Wenji Su[2] · Jiaqi Lu[2] · Sophie Gong[2] · Georg C. Terstappen[2,] · Ru Zhang[1] · Wandong Zhang[2,4,]

Received: 17 October 2018 / Accepted: 2 February 2019 / Published online: 11 May 2019

Abstract An *in vitro* blood-brain barrier (BBB) model is critical for enabling rapid screening of the BBB permeability of the drugs targeting on the central nervous system. Though many models have been developed, their reproducibility and renewability remain a challenge. Furthermore, drug transport data from many of the models do not correlate well with the data for *in vivo* BBB drug transport. Induced-pluripotent stem cell (iPSC) technology provides reproducible cell resources for *in vitro* BBB modeling. Here, we generated a human *in vitro* BBB model by differentiating the human iPSC (hiPSC) line GM25256 into brain endothelial-type cells. The model displayed BBB characteristics including tight junction proteins (ZO-1, claudin-5, and occludin) and endothelial markers (von Willebrand factor and Ulex), as well as high trans-endothelial electrical resistance (TEER) (1560 $\Omega.cm^2 \pm$ 230 $\Omega.cm^2$) and γ-GTPase activity. Co-culture with primary rat astrocytes significantly increased the TEER of the model (2970 $\Omega.cm^2$ to 4185 $\Omega.cm^2$). RNAseq analysis confirmed the expression of key BBB-related genes in the hiPSC-derived endothelial cells in comparison with primary human brain microvascular endothelial cells, including P-glycoprotein (Pgp) and breast cancer resistant protein (BCRP). Drug transport assays for nine CNS compounds showed that the permeability of non-Pgp/BCRP and Pgp/BCRP substrates across the model was strongly correlated with rodent *in situ* brain perfusion data for these compounds (R^2 = 0.982 and R^2 = 0.9973, respectively), demonstrating the functionality of the drug transporters in the model. Thus, this model may be used to rapidly screen CNS compounds, to predict the *in vivo* BBB permeability of these compounds and to study the biology of the BBB.

Keywords Blood-brain barrier · Drug transport · Induced pluripotent stem cell · Cell differentiation · Prediction of *in vivo* permeability

Electronic supplementary material The online version of this article (https://doi.org/10.1007/s12264-019-00384-7) contains supplementary material, which is available to authorized users.

✉ Georg C. Terstappen
georg.c.terstappen@gsk.com; georg.terstappen@gmail.com

✉ Ru Zhang
ru.zhang@tongji.edu.cn

✉ Wandong Zhang
wzhan2@uottawa.ca; wandong.x.zhang@gsk.com

[1] Shanghai Key Laboratory of Signaling and Disease Research, Laboratory of Receptor-Based Bio-medicine, Collaborative Innovation Center for Brain Science, School of Life Sciences and Technology, Tongji University, Shanghai 200092, China

[2] Platform Technology & Sciences, GlaxoSmithKline China R&D Centre, Shanghai 201203, China

[3] Neurosciences Therapeutic Area Unit, GlaxoSmithKline China R&D Centre, Shanghai 201203, China

[4] Human Health Therapeutics Research Centre, National Research Council of Canada; Faculty of Medicine, University of Ottawa, Ottawa K1A0R6, Canada

Introduction

Evaluation of the BBB permeability of potential drug molecules is important in the context of central nervous system (CNS) drug discovery. Sufficient amounts of drug molecules are needed to penetrate the BBB and reach targets in CNS for effective treatment of CNS diseases. A variety of BBB modeling methodologies for assessing and predicting CNS drug penetration have been developed [1, 2]. Combinations of *in silico* prediction, cell-culture

models, and animal *in vivo* studies are commonly used for CNS drug candidate selection [3, 4]. Among these, cell-based models serve as a crucial tool for transporter-substrate confirmation, permeability testing and prediction, and efflux ratio estimation. Significant efforts have been devoted to establishing an ideal cellular model that is easily scalable, predictable and consistent, and resembles *in vivo* BBB characteristics [2, 5–7]. Many *in vitro* cellular models have been developed based on primary brain endothelial cells or immortalized cell lines [6, 7]. However, the endothelial monolayer of many models is not well sealed by tight junctions, leading to low trans-endothelial electrical resistance (TEER), paracellular leakage, and/or loses functional gene expression and cellular polarity of the original brain endothelial cells during culture and passage. Thus, those models may not predict *in vivo* CNS drug BBB permeability well. For human *in vitro* BBB models, the availability of primary human cells and relevant ethical issues restrict their application, particularly by pharmaceutical companies for large-scale drug screening. For animal *in vitro* BBB models, species differences and resource demands limit their application in drug discovery [6].

The introduction of human induced pluripotent stem cell (hiPSC) technology has provided an unprecedented tool for regenerative medicine and disease modeling [8–10]. Several reports have shown that iPSC-derived endothelial cells (ECs) can supply scalable, renewable, and unlimited human-relevant resources for *in vitro* modeling [11, 12]. HiPSC-derived *in vitro* BBB models developed from the hiPSC line IMR90-4 by Lippmann and colleagues show highest TEER (3000 $\Omega.cm^2$ – 5300 $\Omega.cm^2$) in the presence of retinoic acid (RA), pericytes, and neural progenitor cells [11, 13]; while another stem cell-derived model has a low TEER (100 $\Omega.cm^2$ – 180 $\Omega.cm^2$) [14]. Recently, a human amniotic fluid stem cell-derived *in vitro* BBB model was established with an average TEER of $\sim$500 $\Omega.cm^2$ and the addition of human astrocyte-conditioned media or RA increased it to 1090 $\Omega.cm^2$ and 1528 $\Omega.cm^2$, respectively [15]. The model has been used to study antibody-triggered receptor-mediated transcytosis [15]. Katt and colleagues established an *in vitro* BBB model from the BC1 iPSC line and the TEER values reached 1780 $\Omega.cm^2$ – 1920 $\Omega.cm^2$ [16]. Many of the *in vitro* models have been tested and analyzed for drug permeability properties but have not been compared with *in situ* brain perfusion data from animal studies. In this report, the hiPSC line GM25256 was differentiated into human endothelial-type cells using a protocol modified from Lippmann *et al.* [11, 13]. After optimization and evaluation of the BBB characteristics of the differentiated EC cells, co-cultures with primary rat glial cells resulted in a robust human *in vitro* BBB model. We performed drug transport assays for nine typical clinical drugs using this model and compared the results with rodent *in situ* brain perfusion data for those drugs. Our results showed that the *in vitro* results from our model are highly predictable of the *in vivo* BBB permeability of the compounds.

Materials and Methods

Chemicals and Materials

Cell culture plates and transwell inserts (24-well format, 1 μm or 0.4 μm pore size) were from Millipore Inc. (Bedford, MA). Cell culture reagents were from Life Technology (Carlsbad, CA). Chemicals were from Sigma (St. Louis, MO) unless otherwise indicated. The human iPSC line GM25256 was obtained from the National Institute of General Medical Sciences Human Genetic Cell Repository at Coriell Institute for Medical Research (Camden, NJ) and was generated from skin fibroblasts (male, 30 years old at sampling). Primary human brain microvascular endothelial cells (HBMECs) were from ScienCell (Carlsbad, CA) and maintained in the EndoGRO^{TM}-MV Complete Medium Kit supplemented with 1 ng/mL fibroblast growth factor 2 (Millipore, Burlington, MA).

Cell Culture and Differentiation

Human iPSC GM25256 cells were maintained on Matrigel (Fisher Scientific, Hampton, NH) in mTeSR1 medium (StemCell Technologies, Vancouver, Canada), passaged by Accutase (StemCell Technologies), and mechanically dissociated to lift the cells from culture dishes/flasks. HiPSC cells were counted using Nucleocounter (ChemoMetec, Ronkonkoma, NY). Cells were differentiated using a protocol modified from Lippmann *et al.* [11, 13]. After culture for 6 days in unconditioned medium [Dulbecco's Modified Eagle Medium (DMEM)/Ham's F-12, Life Technologies, Carlsbad, CA] containing 20% Knockout Serum Replacement (KOSR) (Life Technologies), 1% minimum essential medium Non-Essential Amino Acid Solution (Life Technologies), 1% L-glutamine (Life Technologies), and 0.836 μmol/L β-mercaptoethanol (Sigma), the culture medium was switched to endothelial medium [(EM; Human Endothelial-Serum-free Medium (SFM), Life Technologies)] supplemented with 1% platelet-poor derived serum (PDS) (Biomedical Technologies, Stoughton, MA) and 20 ng/mL basic fibroblast growth factor (bFGF; Life Technologies) with 20 μmol/L RA (Sigma) and 1.3 μmol/L hydrocortisone (Sigma). The medium was changed every other day, and after 13 days in EM, the differentiated ECs were passaged using Versene and mechanical dissociation and plated onto 24-well Transwell culture inserts coated with 400 μg/mL collagen

(Sigma-Aldrich, St. Louis, MO) and 100 μg/mL fibronectin (Life Technologies) overnight. The cells were cultured on the inserts for up to 3 days in EM−1% PDS medium (including Human Endothelial-SFM, 1% PDS, 20 ng/mL bFGF, 20 μmol/L RA, and 1.3 μmol/L hydrocortisone) in the presence of rat glial co-culture (see below). Alternately, the differentiated ECs were placed on 96-well plates (Corning, MA) coated with 400 μg/mL collagen IV and 100 μg/mL fibronectin for immunocytochemistry experiments.

Animals

The use of animals in this study was conducted in accordance with the GlaxoSmithKline (GSK) Policy on the Care, Welfare and Treatment of Laboratory Animals and had been reviewed and approved by the Institutional Animal Care and Use Committee at the GSK R&D China, Shanghai. The neonatal Sprague–Dawley rat pups (postnatal days 0 – 2) were housed under standard environmental conditions (ambient temperature 21°C, humidity 60%, 12 h:12 h light/dark cycle) with *ad libitum* access to food and water. Rat primary glial cells were generated and cerebral capillary depletion were carried out as described below.

Primary Rat Cortical Astroglial Culture

The primary rat cortical astroglial cell cultures were prepared following a published protocol [17]. Briefly, the brain of each postnatal rats was removed and cortical regions were dissected. After removal of the meninges, the hemispheres were cut into small pieces and digested with 0.25% Trypsin-EDTA (Life Technologies, CA). The cell suspension was filtered through a 40-μm cell strainer (BD Bioscience, Franklin Lakes, NJ) and centrifuged at 4°C for 5 min at 200 × g. The supernatant was discarded and the cell pellet re-suspended in DMEM with 10% fetal bovine serum, 1% GlutaMAX-I, and 1% PenStrep (all from Life Technologies). Then the cells were diluted in complete medium to the required density for seeding in T-175 flasks coated with 50 μg/mL poly-D-lysine (Millipore, Boston, MA) for 1 h at 37°C. The medium was changed every 3–4 days until day 7, when the flasks were shaken at 200 rpm in a CO_2 incubator for 2 h to remove the oligodendrocytes. The supernatant was discarded and the cells were re-plated into 24-well plate coated with poly-D-lysine at 1×10^5 cells/well. Cells were ready to use at 48–96 h after seeding.

Cerebral Capillary Depletion

The cerebral capillaries from rat brain were prepared following Triguero's protocol [18]. Three rats were used in the capillary depletion. Briefly, rats were euthanized with isoflurane, the brain was removed, and one hemisphere was homogenized with a Dounce tissue-grinder (20 strokes) in 500 μL Dulbecco's phosphate-buffered saline (DPBS; Life Technologies) with a protease inhibitor cocktail (Sigma, St. Louis, MO). Dextran (1 mL of 26%) was added with the protease inhibitor cocktail (Sigma, St. Louis, MO), and the final dextran concentration reached at least 13%. The homogenate was then vortexed and homogenized again (3 strokes), and an aliquot of 500 μL was kept as a negative control. The rest of the homogenate was centrifuged at 5400 × g at 4°C for 15 min; the supernatant was removed and kept as another control. The pellet (capillary fraction) was suspended in 0.5 mL DPBS with protease inhibitor cocktail (Sigma, St. Louis, MO). The pellets and the whole-brain homogenates were sonicated and then used for assays.

Immunocytochemistry and Confocal Microscopy

The cells were washed once with DPBS and fixed in 4% paraformaldehyde (ThermoFisher, Waltham, MA) in DPBS for 30 min. After three washes with DPBS, the cells were permeabilized and blocked with 0.1% Triton X-100 in blocking buffer (ThermoFisher, Pittsburgh, PA) for 1 h. All antibody solutions (Table S1) were prepared in blocking buffer. Cells were incubated at 4°C with 10 μg/mL primary antibody overnight. After three washes with DPBS, the cells were incubated for 1 h with 4 μg/mL secondary antibody (Life Technologies). The cells were washed three times in DPBS and incubated with 300 nmol/L DAPI (Life Technologies) in DPBS for 10 min, followed by three DPBS washes and visualization. All immunocytochemistry was performed on cells after two days of culture on 96-well plates. Images were captured with a 20× or 40× objective lens on a Zeiss LSM 710 confocal microscope (Leica-microsystems, Thornwood, NY).

Cell Imaging

Images of cells stained with primary and secondary antibodies were captured and quantified using a Cellomics ArrayScan VTI 700 (ThermoFisher, Pittsburgh, PA). Negative controls were cells stained with secondary antibody only.

γ-Glutamyl Transpeptidase (γ-GTPase) Activity Assay

γ-GTPase activity assays were conducted on iPSC-derived endothelial cells, isolated rat cerebral microvessels, and brain homogenates using a γ-GTPase activity kit (Sigma). Three passages of iPSC-derived endothelial cells were used

in the assay. Rat cerebral microvessels were isolated from three rats as described above. The isolated vessels and brains were mixed from three rats individually in the assays. The amounts of protein in the samples were quantified using a BCA Protein Assay kit (ThermoFisher, Pittsburgh, PA). Equal amounts of proteins from each sample were used for the γ-GTPase assays, following manufacturer's instructions.

Trans-endothelial Electrical Resistance Measurement

The TEERs of the cell monolayers of the *in vitro* BBB model were measured using Millicell ERS-2 Voltohmmeter (Millipore, Burlington, MA). The resistance of a blank culture transwell coated with collagen IV and fibronectin was measured and subtracted from each experimental value. The resulting value was multiplied by the total membrane surface area to obtain the TEER value in $\Omega \cdot cm^2$. TEER values were measured for all drug transport assay wells and for different passages following the manufacturer's guide as described (http://www.emdmillipore.com/CA/en/product/Millicell-ERS-2-Voltohmmeter,MM_NF-MERS00002). Leaking wells were eliminated from the analysis.

Drug Transport Assays

Drug transport studies were performed as described previously [19, 20]. All the transwells for drug transport assays were prepared under optimized conditions with rat glial co-culture. In brief, the transport of test compounds (0.6 μmol/L) was measured in one (apical-to-basolateral) or two (apical-to-basolateral and basolateral-to-apical) directions in the presence or absence of a transporter inhibitor. The transport medium was DMEM supplemented with 4500 mg/L D-glucose, 4 mmol/L L-glutamine, and 25 mmol/L HEPES but without sodium pyruvate and phenol red, pH 7.4. The incubation time was 90 min. Lucifer Yellow (LY) (Promega Inc., Madison, WI) was used as a paracellular marker to monitor the integrity of the iPSC-derived endothelial monolayer. LY was added to the top chamber of the transwell at a final concentration of 100 nmol/L. The assays were conducted following manufacturer's instructions. Monolayers with permeability to LY > 50 nm/s were considered leaky and excluded from further analysis. The exact permeability (P_{exact}) to LY and test compounds was determined using the equation we described previously [20]. Drug transport assays were carried out using three independent differentiation passages of iPSC-derived endothelial cells. The P_{exact} (nm/s) for each test drug was calculated as follows:

$$P_{exact} = -\left(\frac{V_D V_R}{(V_D + V_R)At}\right) \ln\left\{1 - \frac{(V_D + V_R)C_R(t)}{((V_D C_D(t) + V_R C_R(t))}\right\} \times 10^7$$

where V_D and V_R are donor and receiver well volumes in mL, respectively; A is the membrane surface area in cm^2; t is transport time in seconds; $C_R(t)$ and $C_D(t)$ are the measured mass spectrometric response or concentration of test compound in the receiver and donor wells at time t (90 min), respectively [20].

Analysis of Drug Compounds in Biological Samples

LY was quantified using a Spectramax Gemini cytofluorimeter (Molecular Devices, Silicon Valley, CA) with excitation at 430 nm and emission at 540 nm. Quantification of other compounds was carried out using Waters Acquity™ ultra performance liquid chromatography (UPLC) (Milford, MA) coupled with an Applied BioSystems API4000 Qtrap tandem mass spectrometry system (UPLC-MS/MS; Foster City, CA). The chromatographic separation was achieved on a Waters Acquity UPLC™ BEH C18 analytical column (50 × 2.1 mm, 1.7 mm) at 40°C, using a gradient of aqueous (A: 1 mmol/L ammonia acetate in water) and organic [B: CH_3CN-CH_3OH (4:1, v/v)] mobile phases at 500 μL/min. The elution gradient was: 0 min at 25% B; 0–1.4 min ramped to 90% B; 1.4 min – 1.8 min maintained at 90% B; 1.8–1.85 min down to 25% B; and 1.85–2.5 min held at 25% B. The run-time for each compound was 2.5 min. Detection by tandem MS in positive electrospray ionization mode was based on precursor ion transitions to the strongest intensity production under optimized mass spectrometric settings. The multiple reaction monitoring transitions used for quantitative analysis were as follow: *m/z* 280.1→234.9 for doxepin; 438.3→171.0 for fluphenazine; 325.7→262.1 for citalopram; 267.2→145.1 for atenolol; 327.2→192.5 for clozapine; 253.1→117.3 for cimetidine; 384.1→230.8 for prazosin; 411.3→191.0 for risperidone; and 300.6→184.0 for metoclopramide (for MS transitions, see Table 1).

RNA-seq and Data Analysis

Total RNA was extracted from cells with TRIzol (Invitrogen, Carlsbad, CA) and all RNA integrity number values were > 8.2. RNA-Seq libraries were synthesized with 1 μg RNA following the Illumina TruSeq mRNA sample preparation v2 protocol (Illumina, San Diego, CA). The library was quantified using a Qubit 2.0 fluorimeter (Invitrogen). Sequencing was carried out using a 2 × 150-bp paired-end configuration. Image analysis and base calling were conducted by the HiSeq Control Software

Table 1 MS transitions

Compound Name	MRM	DP	CE	CXP	Dwell Time (ms)
SB243213 (Internal standard, Pos)	429.2/228.2	103	36	10	50
Caffeine	195.2/138.0	50	20	10	50
Doxepin	280.1/234.9	81	25	10	50
Fluphenazine	438.3/171	100	35	10	50
Citalopram	325.7/262.1	90	28	10	50
Atenolol	267.2/145.1	75	37	10	50
Clozapine	327.2 /192.5	105	61	10	50
Cimetidine	253.1 →117.3	62	21	10	50
Prazosin	384.1 /230.8	90	58	10	50
Risperidone	411.3/191.0	92	42	10	50
Metoclopramide	300.6/184.0	73	43	10	50

MRM: Multiple Reaction Monitoring; DP: Declustering Potential; CE: Collision Energy; CXP: Collision Cell Exit Potential.

(HCS) + OLB + GAPipeline - 1.6 (Illumina, San Diego, CA) on the HiSeq instrument.

Cryopreservation of hiPSC-derived Endothelial Cells

Freshly-differentiated ECs were cryopreserved following a published protocol [21] with minor modifications during the freezing and recovery of cells. The freezing medium contained 10% dimethyl sulfoxide (DMSO) and 30% FBS (Life Technologies –Thermo Fisher Scientific., CA) in EC medium. The recovered cells were grown under optimized conditions as described above and examined for the EC marker Ulex and the tight junction marker ZO-1. The *in vitro* BBB model composed of recovered cells co-cultured with primary rat glial cells was assessed for TEER values and Lucifer Yellow permeability.

Statistical Analysis

All values are presented as mean ± SD, and *P*-values were assessed by unpaired, two-tailed, Student's *t* test, using Prism version 7 (GraphPad Software, La Jolla, CA) unless otherwise indicated. $P < 0.05$ was considered statistically significant. Exact passages and *n* values are shown in the figure legends.

Results

Differentiation and Characterization of Human iPSC Line GM25256 into Endothelial Cells

The hiPSC GM25256 cells were first characterized by immunofluorescence staining for pluripotency-associated markers, such as OCT4 and TRA1-60 (Fig. S1A, B). Imaging analysis showed that 99.52 ± 0.09% of the cells were OCT4 positive, and 82.81 ± 8.8% were TRA1-60 positive (Fig. S1C). The GM25256 cells were then differentiated in unconditioned medium (UM) for 6 days, matured in EM for 13 days, purified by sub-culturing on a collagen IV- and fibronectin-coated surface. The progression of the differentiation process and morphology of the cells are shown in Fig. 1A and B. The characteristic features of iPSC differentiation into ECs included the formation of tight junctions and the expression of EC markers, *i.e.*, von Willebrand factor (VWF) and *Ulex europeas* agglutinin I (Fig. 1C). The tight-junction markers ZO-1, claudin-5, and occludin, were nicely expressed in the monolayer of hiPSC-derived ECs and co-localized to cell-cell junctions (Fig. 1D). Ulex and VWF were positive in the ECs (Fig. 1C). The positive expression of tight-junction and endothelial markers confirmed the endothelial nature of the cells differentiated from hiPSC GM25256 cells. Thus, enriched hiPSC-derived ECs were successfully generated by the modified protocol [11, 13]. In addition to EC and tight junction markers, the cells also expressed receptors and transporters found on brain endothelial cells, including transferrin receptor (TfR), insulin-like growth factor-1 receptor (IGF1R), low density lipoprotein receptor-related protein 1 (LRP1), solute carrier (SLC) family 3 member 2/CD98 heavy chain (SLC3A2/CD98hc), SLC2A1/glucose transporter-1 (GLUT-1), ABCB1/P-glycoprotein (Pgp), ABCC1/multidrug resistant protein-1 (MRP1), and ABCG2/breast cancer resistant protein (BCRP) (Figs. 1E and 2A–C). The hiPSC line was differentiated into EC cells for > 20 passages. The phenotype and the expression of EC biomarkers were generally consistent with low inter-passage variation if the protocol was strictly followed. It should also be noted that

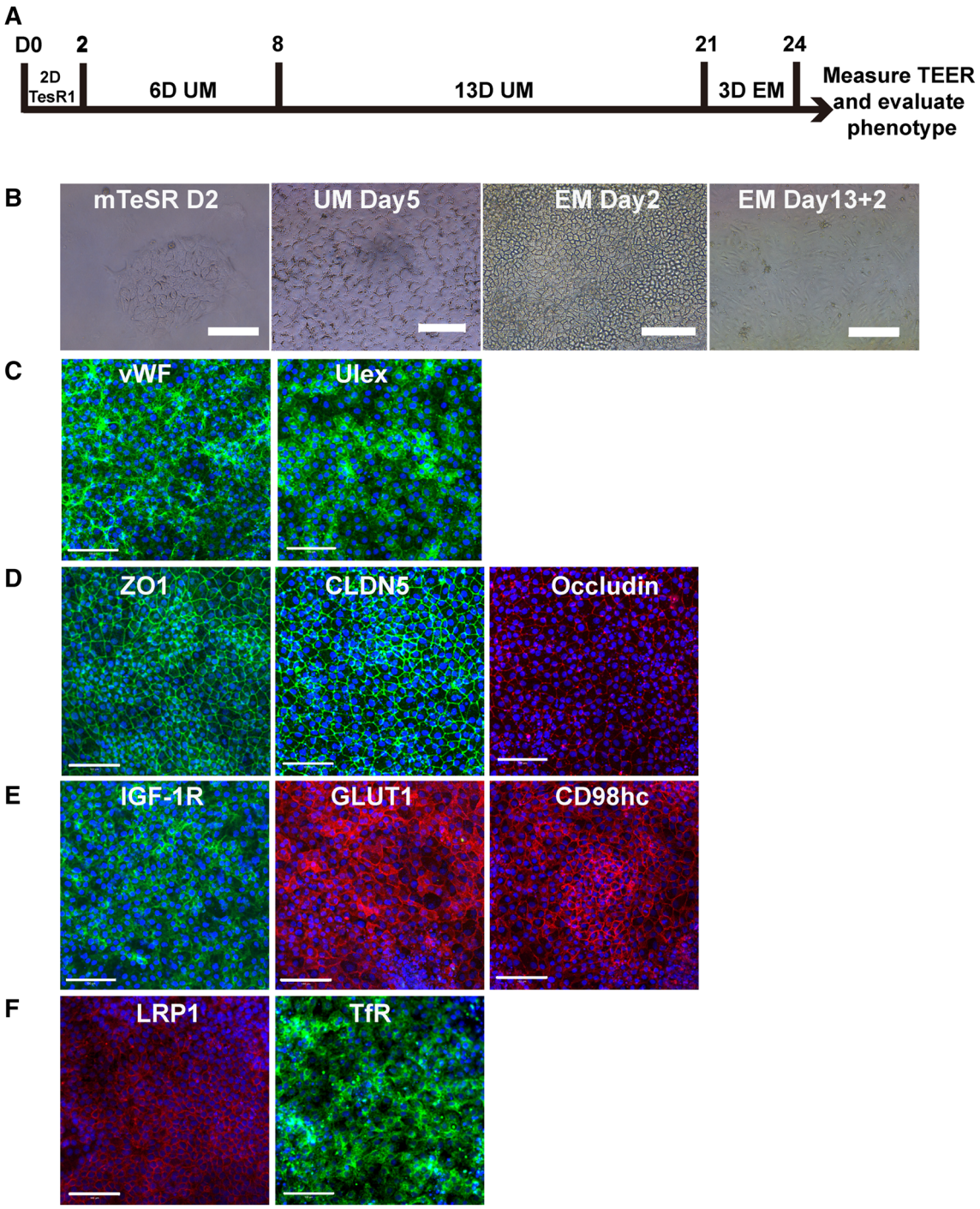

Fig. 1 Differentiation and characterization of hiPSC-derived endothelial cells (ECs). **A** Schematic of the differentiation process. **B** Phase-contrast images of hiPSC cells at different differentiation stages, including 2 days in mTeSR, after 5 days in unconditioned medium culture, after 2 days in EM culture, and after 2 days of subculturing. **C** Expression of EC markers VWF (green) and Ulex (green). **D** Expression of tight-junction markers ZO-1 (TJP1) (green), claudin-5 (CLDN-5) (green), and occludin (OCLN) (red). **E** Expression of receptors and transporters IGF-1R (green), GLUT-1 (red), CD98hc (red), LRP1 (red), and transferrin receptor (TfR) (green). Scale bar, 100 μm for **B**, **C**, **D**, and **E**.

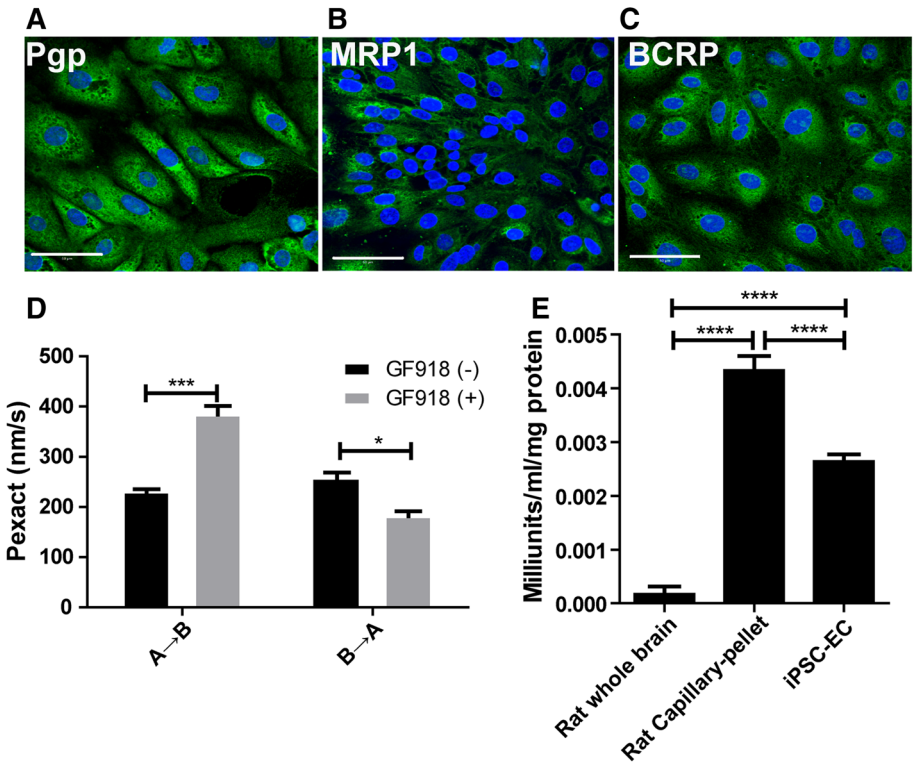

Fig. 2 Expression of drug transporters, drug transport assays, and γ-GTPase in hiPSC-derived *in vitro* BBB model. Drug transporters were expressed in hiPSC-derived ECs. **A** Pgp (green), **B** MRP1 (green), and **C** BCRP (green). Scale bar, 100 μm for **A**, **B**, and **C**. **D** Inhibition of efflux transporter by GF120918 (three passages, n = 6/passage). The permeability of Loperamide (a Pgp substrate) across the *in vitro* BBB model showed a significantly increased in the presence of the Pgp inhibitor GF120918 (from apical to basolateral, A to B; $^{***}P < 0.001$, unpaired two-tailed t-test). The directional pumping was also significantly decreased in the presence of GF120918 (from basolateral to apical, B to A; $^{*}P < 0.05$, unpaired two-tailed t-test). **E** Activity of γ-glutamyl transpeptidase (γ-GTPase) to evaluate the metabolic enzyme in hiPSC-derived ECs in comparison with rat cerebral capillaries and whole-brain homogenates. Cerebral capillaries (pellet fraction) were isolated from rat brains as a positive control using a published protocol, and the whole-brain homogenates were also used as a control. γ-GTPase was highly active in the pellet of rat cerebral capillaries ($^{****}P < 0.0001$, unpaired, two-tailed t-test; n = 6). The activity of γ-GTPase was significantly higher in hiPSC-derived ECs than in rat brain homogenates, but lower than in rat cerebral capillaries ($^{****}P < 0.0001$, unpaired, two-tailed t-test; n = 6).

the differentiation of the cells in EM was 13 days in our modified protocol (Fig. 4A) as compared to 2 days in Lippmann *et al*. [11, 13] and 10 days in Ribecco-Lutkiewicz *et al*. [15]. Different iPSC lines may have different biological properties so that the differentiation protocols need to be modified to obtain the best results for the iPSC lines used.

γ-Glutamyl Transpeptidase Activity in hiPSC-derived Endothelial Cells

One of the characteristics of cerebral microvascular and capillary endothelial cells is that they produce highly active metabolic enzymes known as the metabolic barrier of the BBB, such as alkaline phosphatase, γ-glutamyl transpeptidase (γ-GTPase), and cholinesterase, among others [22, 23]. These enzymes may play a role in detoxifying or modifying drugs/neurotoxic agents that enter the BBB cells. We measured the level of γ-GTPase in hiPSC-derived ECs using a γ-GTPase activity kit. Rat brain homogenates and isolated cerebral capillaries (pellet) were mixed individually from three rats and used as controls in each of the assays. Three passages of hiPSC-derived ECs were used in the assays. The number of hiPSC-derived ECs could be counted and correlated with the levels of γ-GTPase activity, but it was difficult to count the number of cells in rat brain tissue and capillary fractions. Thus, equal amounts of protein from rat brain homogenates, cerebral capillaries, and iPSC-derived ECs were used in the assays for comparison. The activity of γ-GTPase was significantly higher in the cerebral capillary (pellet) fraction than in the brain homogenates. The activity of the enzyme in hiPSC-derived ECs was significantly higher than in the brain homogenates, but significantly lower than in the brain capillaries (Fig. 2E; $n = 6$; $P < 0.0001$, unpaired, two-tailed t-test). This also confirmed the brain endothelial nature of the hiPSC-derived cells although their γ-GTPase activity was lower than that of rat brain capillaries.

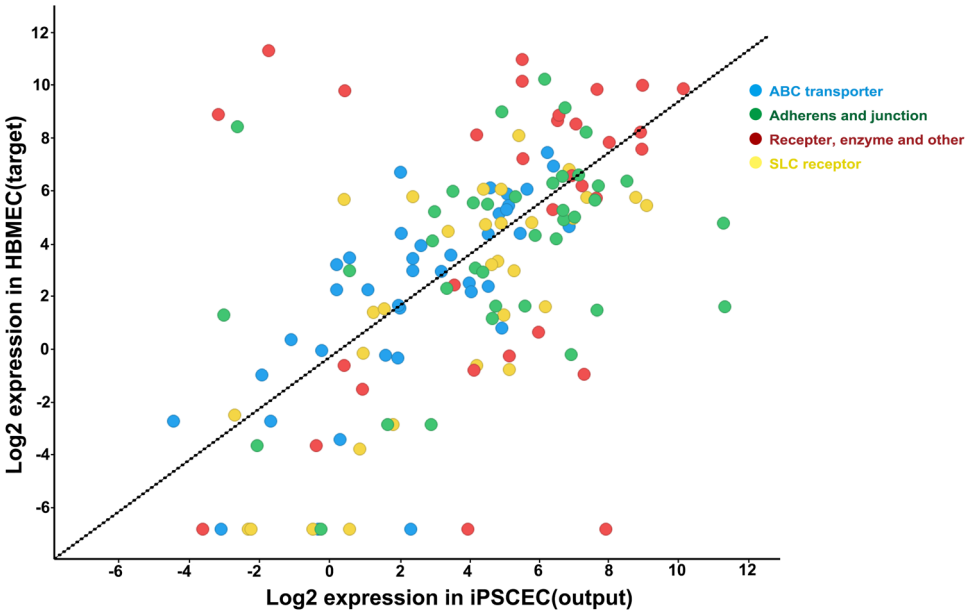

Fig. 3 RNA-seq analysis of hiPSC-derived endothelial cells compared with primary human brain microvascular endothelial cells (HBMECs). Correlation of ATP-binding cassette (ABC) transporters (blue), solute carrier (SLC) transporters (yellow), adherens and tight junction protein (green), receptors, and enzyme (red) in hiPSC-derived ECs *versus* those from primary HBMECs.

RNA-seq Analysis

HBMECs derived from human brain cortex were obtained from ScienCells Research Laboratories (Carlsbad, CA). The cells were characterized by ScienCells as expressing BBB biomarkers. HBMECs and hiPSC-derived ECs were harvested and RNA samples were extracted for RNA-seq analysis as described above. The quality of RNA-seq data was evaluated by FastQC as the phred score, base composition, k-mer content, and 5' and 3' bias. Using the gene annotation of ENSEMBL (GRCH38.p10), counts per gene were quantified using a tool implemented in the R SubRead package. The counts were normalized using a quantile normalization method implemented in the edgeR package. The log2-transformed median values were calculated to indicate the overall expression levels of cells. The differential expression was analyzed using DESeq2 and then all of the differentially-expressed genes were selected at a cutoff of adjusted P value <0.01. The gene expression pattern of marker genes was visualized for their expression status in different cell types. BBB-related genes as described in the literature [24], including ATP-binding cassette transporters, SLC transporters, adherens and junctions proteins, receptors, and enzymes were analyzed between hiPSC-derived ECs and HBMECs. Many of the key BBB genes, such as ABCB1/Pgp, ABCC1/MRP-1, TJP1 (ZO-1), ABCC4/MRP-4, and ABCG2/BCRP, were correlated very well between HBMECs and iPSC-derived ECs (Fig. 3). This analysis showed that the patterns of the key BBB genes expressed in hiPSC-derived ECs were similar to those of HBMECs.

Optimization of the hiPSC-derived *in vitro* BBB Model

A high TEER value is a hallmark of the *in vivo* BBB and represents its integrity and the biophysical barrier [6]. Most of the *in vitro* BBB models have low TEER values and the paracellular space of the endothelial monolayer is not tightly sealed compared with *in vivo* BBB conditions [6]. Our *in vitro* BBB model and its TEER value were optimized under different conditions, such as sub-culture in different conditions, culture time (24 h to 96 h), cell density (1 to 8 $\times$ 10^5 cells/insert), and different medium components (1% PDS, 5% KOSR, RA, and hydrocortisone) with or without rat primary astroglial co-culture, and the pore size of tissue culture inserts (Fig. 4A–F). The primary astroglial cells generated for this study were characterized by immunofluorescence staining and confirmed to be positive for neuron-specific class III β-tubulin (Tuj1) (Fig. S1I) and astrocyte-related markers including GFAP and s100β (Fig. S1G, H). Imaging analysis showed that GFAP-, S100β-, and Tuj1-positive cells were 67.40 $\pm$ 11.3%, 84.46 $\pm$ 11.65%, and 2.65 $\pm$ 1.31%, respectively (Fig. S1J). This confirmed that most of the primary cell cultures were astroglial cells. Two compounds were tested to enhance the BBB properties and further optimize the protocol. RA was added into the medium to enhance the TEER value as described [11]. The TEER was significantly increased in the presence of RA (20 µmol/L) (Fig. 4B; three passages, n = 4/passage; P <0.0001, unpaired two-tailed t-test) as reported [11]. We also added hydrocortisone (1.3 µmol/L) to enhance the barrier properties of the model [25–27]. Hydrocortisone alone did not have a significant effect on TEER, but when RA and

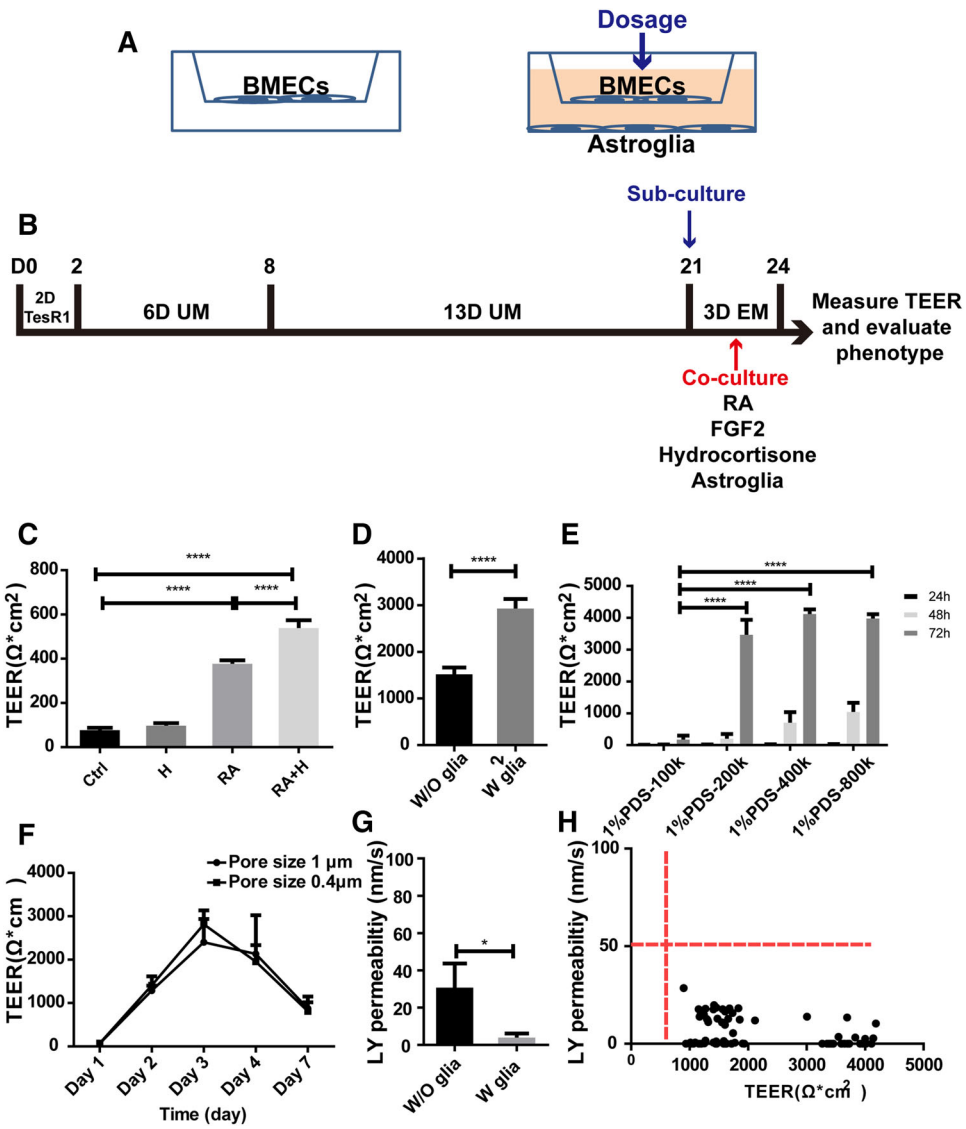

Fig. 4 Optimization of the *in vitro* BBB model. **A**–**E** Optimization of timing, subculture medium, cell density, time, and insert pore size to optimize the TEER value in the human iPSC-derived model. **B** Effects of retinoic acid (RA; 20 μmol/L) and hydrocortisone (H; 1.3 μmol/L) on TEER. **C** Effects of rat glial co-culture on TEER in the presence of retinoic acid (20 μmol/L) and hydrocortisone (1.3 μmol/L). **D** Effects of 1% PDS, the number of seeding cells, and timing on TEER in the presence of retinoic acid, hydrocortisone, and rat glial co-culture. **E** Effect of pore size of culture inserts (0.4 μm and 1.0 μm) and timing on TEER. **F** Permeability of Lucifer yellow (LY) across the model with or without rat astroglial cell co-culture. **G** Permeability of Lucifer yellow remained stable when the TEER threshold was between 1000 (without glial co-culture) and 4000 (with glial co-culture) Ω.cm^2. All the data were from 3 batches of differentiated cells. Error bars represent SD (****P <0.0001, ***P <0.001, *P < 0.05, unpaired, two-tailed t-test). For **G**, the data were obtained from three batches of differentiated cells and one dot represents one transwell.

hydrocortisone were added together, the TEER was significantly enhanced (Fig. 4B; three passages, n = 4/passage; $P < 0.001$, $P < 0.0001$, unpaired, two-tailed t-test). Thus, the combination of RA and hydrocortisone was used in our modified protocol to enhance the TEER and biophysical barrier properties of the model. Two culture medium conditions containing 1% PDS (Fig. 4D) and 5% KOSR (data not shown) after sub-culture were each tested for their effects on TEER. Other conditions, including 1 × 10^5, 2 ×10^5, 4 ×10^5, and 8 × 10^5 cells/insert, and the timing (24 h to 72 h) post-subculture, were also tested, separately and in combination, to optimize the conditions for TEER (Fig. 4D). Those conditions (RA, hydrocortisone, bFGF, 1% PDS, and 4 ×10^5 cells/insert) were sufficient to reach the highest TEER values in the absence of rat glial co-culture (Fig. 4C; three passages, n = 6/passage) at 1560 Ω.cm^2 ± 230 Ω.cm^2. To induce and enhance the BBB properties of the model, co-culture with

primary rat glial cells was tested in addition to the conditions described above. TEER values significantly increased to 2970 $\Omega.cm^2 \pm 363\ \Omega.cm^2$ with glial co-culture (Fig.4C; three passages, n = 7/passage; P <0.0001, unpaired, two-tailed t-test). Thus, co-culture with rat glial cells significantly increased the biophysical barrier properties of hiPSC-derived cells in the *in vitro* BBB model. The numbers of cells at 1×10^5, 2×10^5, 4×10^5, and 8×10^5 cells/insert and the timing were tested under glial co-culture conditions and in the presence of RA and hydrocortisone (Fig. 4D), and 2 to 8×10^5 cells/insert yielded similar TEER values at 72 h and the maximum TEER reached was 4185 $\Omega \cdot cm^2$ (n = 3). The condition of 4×10^5 cells/insert was selected for subsequent drug transport experiments. The pore size of the inserts (0.4 μm or 1.0 μm) did not affect the TEER value (Fig. 4E), and 1 μm pore size inserts were used in subsequent experiments. For all the conditions tested, the TEER values were highest at 72 h post-subculture and then started to decline at 96 h. All of the subsequent assays used 72-h transwell models. All of the transwell models were measured for TEER, and leaky transwells were eliminated from analysis.

To further evaluate the integrity of the *in vitro* BBB monolayer at the functional level, LY permeability was measured across the model. LY is a small negatively-charged molecule (MW: 444.3 g/mol) and is commonly used to confirm the monolayer barrier integrity of *in vitro* cell models. In our standard transwell assay, the permeability of LY was 21.6 nm/s ± 23.23 nm/s for ECs in the absence of rat glial co-culture, and 4.94 nm/s ± 4.28 nm/s in the presence of the co-culture (Fig. 4F; $P < 0.05$; 3 passages, 6 replicates/passage). The variations of the TEER of the *in vitro* BBB monolayer were measured during LY permeability assays as the medium was changed to transport assay buffer. The TEER varied from 898 $\Omega \cdot cm^2$ to 4185 $\Omega \cdot cm^2$; however, the permeability to LY remained constant at 0.66 nm/s to 9.2 nm/s despite the TEER variations (Fig. 4G). When the TEER was within this range (< 50 nm/s), the permeability of small molecules across the model remained relatively consistent. This indicated that established monolayers with TEER values > 500 $\Omega \cdot cm^2$ may be good enough for testing the permeability of small molecule compounds [28].

The optimized conditions for the iPSC-derived *in vitro* BBB model included the following: 4×10^5 cells/insert, 1 μm pore size insert, and medium containing 1% PDS, 20 ng/mL bFGF, 20 μmol/L RA, and 1.3 μmol/L hydrocortisone. All the transwells were co-cultured with rat glial cells and used at 72 h. The above optimized conditions were used for all subsequent drug transport assays using freshly-differentiated cells. All the transwells were measured for TEER and LY permeability after the transport assays. If any transwell was leaky or the LY permeability was > 50 nm/s, the transwells were eliminated from analysis.

Cryopreservation of hiPSC-derived Endothelial Cells

Differentiation of iPSC cells into ECs took about three weeks in our case. Thus, it took 3–4 weeks to complete one *in vitro* BBB model study. Therefore, cryopreservation of differentiated ECs would be advantageous for large-scale studies or drug screening in industrial settings. In this way, a large quantity of ECs can be differentiated, cryopreserved, and recovered for *in vitro* BBB model assays when required. A published protocol [22] describes a freezing medium [10 % DMSO and 30 % fetal bovine serum in EC medium] for the cryopreservation of differentiated ECs with high recovery rates and similar BBB characteristics. This protocol was applied with minor modifications during freezing and recovery of our iPSC-derived ECs. The recovered cells were positive for the EC marker Ulex and the tight-junction marker ZO-1 (Fig. 5A). The TEER of the *in vitro* BBB model constituted from the recovered cells reached ~2000 $\Omega.cm^2$ at 48 h and maintained this value at 72 h and 96 h after seeding the cells. Figure 5B shows the TEER results for cryopreserved/recovered ECs at 72 h after seeding on the *in vitro* BBB model (three passages, n = 8/passage). The permeability of LY across the model was ~20 nm/s (Fig. 5C; three passages, n = 8/passage). The TEER values of the transwell models constituted from cryopreserved /recovered cells were lower than those from freshly-differentiated cells, possibly due to the cryopreservation medium and the freezing procedure. The mechanism is unknown, but one of potential factors is that the cryopreservation medium contains 10% DMSO which is known to be toxic to cultured blood cells and vascular ECs and reduces cell proliferation [29, 30]. Since the TEER values were > 500 $\Omega.cm^2$ and LY permeability was <50 nm/s, the model constituted from cryopreserved/recovered ECs was acceptable for testing the BBB permeability of CNS compounds.

Drug transport assays across the hiPSC-derived *in vitro* BBB model

The biological properties and the expression of drug transporters for the *in vitro* BBB model were characterized and the culture conditions were optimized as described above. The functionality of drug efflux transporters in the *in vitro* BBB model was then assessed in the transwell two-chamber model by examining the transport of loperamide, a typical Pgp substrate (three passages, n = 6/passage). The permeability of loperamide from the apical-to-basolateral direction (A to B) was determined to be P_{exact} = 232 nm/s

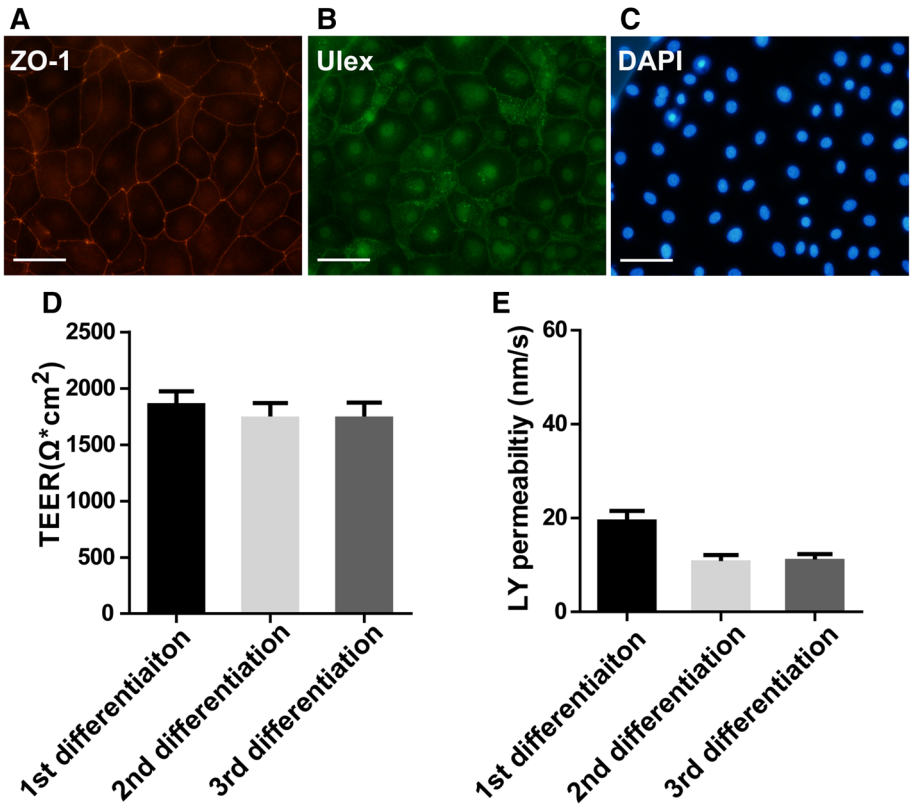

Fig. 5 Characterization of cryopreserved iPSC-derived endothelial cells. **A** Immunocytochemical staining of biomarkers in cryopreserved iPSC-derived ECs: ZO-1 (red), Ulex (green), and DAPI (blue). Scale bar, 100 μm. **B** The TEER reached ~2000 Ω.cm^2 at 48 h after seeding cryopreserved ECs. The TEER was maintained at ~2000 Ω.cm^2 at 72 and 96 h post-seeding. Data for 72 h post-seeding is shown (average ± SD; three passages, n = 8/passage). **C** Permeability of Lucifer Yellow across the *in vitro* BBB model composed of cryopreserved ECs. Three passages of the cells (n = 8/passage) were used in the experiments. The permeability of Lucifer Yellow was ~20 nm/s for the three passages at 72 h post-seeding and there was no statistical difference between them.

± 12.2 nm/s (Fig. 2D). In the presence of the Pgp inhibitor GF120918 (3 μmol/L), the permeability to loperamide was significantly enhanced and the P_{exact} increased to 384 nm/s ± 43.4 nm/s (165.5%↑) (Fig. 2D). Thus, the presence of a Pgp inhibitor significantly inhibited the Pgp-mediated drug efflux (P <0.001, unpaired, two-tailed t-test). Pgp also mediated the directional pumping of loperamide from the basolateral side to the apical side in the *in vitro* BBB model (B to A; 257.92 nm/s ± 25.94 nm/s), and the directional pumping of loperamide from B to A was significantly decreased in the presence of 3 μmol/L GF120918 (Fig. 2D; 181.54 nm/s ± 24.55 nm/s; $P < 0.05$, unpaired, two-tailed t-test). These results demonstrated the functional Pgp-mediated efflux and directional pumping activity in the iPSC-derived *in vitro* BBB model.

Permeability Measurements for Small Molecule Drugs Across the hiPSC-derived *in vitro* BBB Model

To evaluate our hiPSC-derived BBB model for screening new CNS therapeutic agents, we chose 9 drugs with diverse physicochemical and transport properties and available *in situ* rodent brain perfusion data, and examined the permeability of these compounds across our model (Table 2 and Fig. 6). Two groups of drugs were tested, non-Pgp substrates (including passively-diffusing drugs and weak Pgp/BCRP substrates, doxepin, clozapine, fluphenazine, atenolol, and cimetidine) and Pgp/BCRP substrates (risperidone, citalopram, prazosin, and metoclopramide) (Table 2). Atenolol is a passive hydrophilic drug of low BBB penetration *in vivo* (P_e *in situ* = 2.3 nm/s) [31–33] and showed similar penetration across our *in vitro* model (P_{exact} = 11 nm/s). Doxepin and clozapine, which are lipophilic small molecules with passive diffusion properties, exhibited high BBB penetration *in vivo* (P_e *in situ* brain perfusion = 2436 nm/s and 2512 nm/s, respectively) and also showed high penetration across our *in vitro* model (P_{exact} = 448 nm/s and 415 nm/s) (Table 2). It should be noted that the *in vivo* BBB penetration of these compounds was ~5-fold–6-fold higher than in our *in vitro* model [doxepin: P_e *in situ* brain perfusion = 2436 nm/s *vs* our *in vitro* P_{exact} = 448 nm/s (~5-fold difference);

Table 2 Properties of compounds used in drug transport assays

Compound	Pgp/BCRP contribution	P_e *in situ*[#] (nm/s)/ Animal species	Rank order	P_{exact} in hiPSC-derived *in vitro* model (nm/s) (n = 4)	MW (Da)	LogP ($\leq$ 5)
Doxepin	Passive lipophilic	2436/Adult male Sprague-Dawley rats [32]	High	448 ± 22	279	4.08
Clozapine	Passive diffusion	2512/Adult male Sprague-Dawley rats [32]	High	415 ± 30	326	3.67
Risperidone	Strong Pgp (10)*	944/Adult male Sprague-Dawley rats [32]	High	560 ± 9.79	410	3.27
Fluphenazine	Weak Pgp (1.27) *	820/Adult male Sprague-Dawley rats [32]	Medium	149 ± 15	437	4.4
Citalopram	Moderate Pgp (3.13)*	654/Adult male Sprague-Dawley rats [32]	Medium	463 ± 10	324	3.58
Prazosin	Pgp/BCRP (5.2)*	11.3/Mice [31]	Medium	343 ± 23.71	383	1.93
Metoclopramide	Strong Pgp (6.6)*	139/Adult male Sprague-Dawley rats [32]	Medium	323 ± 14.01	299	2.18
Atenolol	Passive hydrophilic	2.3/Mice [31]	Low	11 ± 5	266	0.57
Cimetidine	Pgp/BCRP (+)	2.1/Mice [31]	Low	9.4 ± 0.838	252	0.44

[#]P_e *in situ* data searched from publications of animal studies of *in situ* brain perfusion.

*Brain distributions of the drug in Pgp/BCRP knockout *vs* wild-type animals [38, 39].

MW and Log P of all drugs were obtained from the DrugBank database.

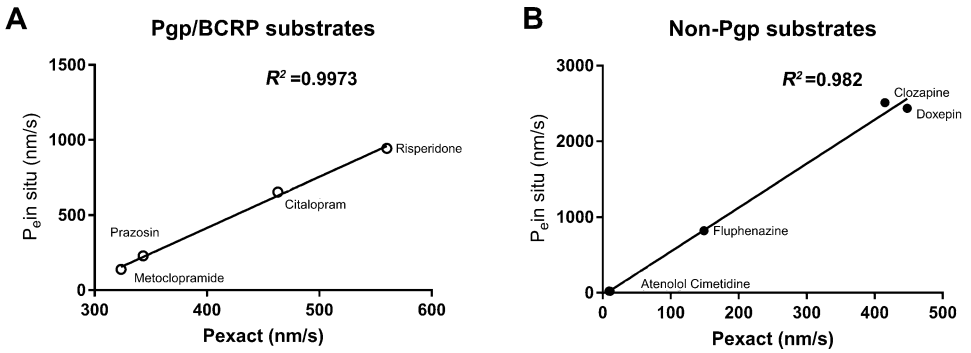

Fig. 6 Characterization of drug permeability in the hiPSC-derived *in vitro* BBB model. All transport studies performed across the *in vitro* BBB model used an optimized condition with rat primary glial co-culture. Correlations between the permeability coefficients of the drugs tested across the *in vitro* BBB model [P_{exact} (nm/s)] and the apparent permeability coefficients of the same drugs measured in rodent models P_e by *in situ* brain perfusion (nm/s) (Table 2). Three passages of iPSC-derived ECs were used in the experiments (n = 6/passage). **A** Linear coefficient of correlation R^2 = 0.9973 for the Pgp substrate drugs risperidone, citalopram, prazosin, and metoclopramide (Prism XY correlation analysis Y = 3.4*X – 945; where X is the P_{exact} obtained from our assay result) (Table 2). **B** Linear coefficient of correlation R^2 = 0.982 for the non-Pgp substrates (including passive-diffusion drugs and weak Pgp/BCRP substrate drugs) clozapine, doxepin, fluphenazine, altenolol, and cimetidine (Prism XY correlation analysis Y = 5.8*X − 35.37; where X is the P_{exact} obtained from our assay result) (Table 2).

clozapine: P_e *in situ* brain perfusion = 2512 nm/s *vs* our *in vitro* P_{exact} = 415 nm/s (~6-fold difference)]. One potential reason is that the drugs may adsorb or accumulate in cerebral vessels in the *in situ* brain perfusion samples, and the vascular-associated drugs may be accounted for during the measurement; while in the *in vitro* BBB model testing, the drugs measured were purely passed through the *in vitro* model. The lower permeability across human the iPSC-derived model found for the drugs (such as clozapine and doxepin) with high passive permeability of *in situ* brain permeability was also likely due to the culture medium of the *in vitro* model in which the components of the medium (such as the levels of proteins) were different from the blood components, and an unstirred water layer may also reduce the permeability of the compounds across the model [34]. Similar results have been reported for clozapine and doxepin across a rat primary brain endothelial *in vitro* BBB model and the MDCKII-MDR1 cell line [33]. Cimetidine is hydrophilic and fluphenazine is lipophilic, and they are weak substrates of Pgp or/and BCRP. They have limited brain uptake *in vivo* and have lower P_{exact} values *in vitro* (P_{exact} = 9.4 nm/s and 149 nm/s, respectively). For non-Pgp substrate drugs (including those with passive diffusion characteristics or weak Pgp/BCRP substrates), the results from the *in vitro-in vivo* correlation provided a high linear coefficient of correlation (R^2 = 0.982; Fig. 6B and Table 2) which was calculated using the Prism XY correlation analysis formula Y = 5.8*X − 35.37 (where X is the P_{exact}

obtained from our assays). The iPSC-derived *in vitro* BBB model is thus highly predictive for *in vivo* BBB permeability of drugs with predominant passive diffusion characteristics or weak Pgp/BCRP substrates using this formula. For Pgp/BCRP substrates (prazosin, risperidone, citalopram, and metoclopramide), the *in vitro* transport results also correlated well with rodent *in situ* brain perfusion data for these drugs (Fig. 6A; three passages, n = 4/passage) (Table 2). The *in vitro-in vivo* correlation provided a high linear coefficient of correlation (R^2 = 0.9973) using another Prism XY correlation analysis formula (Y = 3.4*X – 945; where X is the P_{exact} obtained from our assays). It should be noted that human data of *in vivo* BBB permeability of those compounds is not available for comparison with our *in vitro* BBB model. The development of CNS drugs is usually tested for BBB permeability in animals. The fact that our *in vitro* model can predict BBB permeability of the above groups of the drugs in animal *in situ* brain perfusion experiments provides a quick and valuable option for determining the developability of the compounds. Thus, new CNS compounds in development may be tested in this model to evaluate their *in vivo* BBB permeability.

Discussion

The main interfaces between the CNS and the peripheral circulation are the BBB and the blood-cerebrospinal fluid barrier. Brain microvascular endothelial cells constitute the tight junction proteins expressed in the BBB, polarized efflux and SLC transporters, and metabolic enzymes govern the biophysical, transport, and metabolic barrier functions of the *in vivo* BBB. The combination of physical, biochemical and metabolic barrier functions entails that the *in vivo* BBB characteristics and properties are quite distinct and difficult to mimic *in vitro*. Furthermore, the limited availability of human primary brain endothelial cells does not allow the use of *in vitro* human BBB models for large-scale drug discovery studies and screening efforts. Human iPSC lines can be differentiated to generate ECs with good barrier properties and to generate other types of cells, such as astrocytes, pericytes, and neural precursor cells for human *in vitro* BBB modeling. Thus, hiPSC-derived ECs and other types of cells provide renewable and scalable sources for in *vitro* BBB modeling, drug discovery, and screening. In our work, the hiPSC line GM25256 generated from skin fibroblasts was differentiated into ECs using a modified protocol from which an *in vitro* human BBB model was constituted. Those cells showed BBB structural and functional properties, most importantly well-organized tight junctions at the structural and morphological level, including the expression of the tight junction markers ZO-1, claudin-5, and occludin. At the functional level, the barrier integrity was represented by high TEER values and low paracellular permeability to LY. In fact, the TEER of this hiPSC-derived model system reached 1560 ± 230 $\Omega.cm^2$ in the presence of RA and hydrocortisone without rat glial co-culture. Lippmann and colleagues reported that RA substantially increases the expression of vascular endothelial cadherin in differentiated ECs before passage and purification [11]. Mizee and colleagues showed that RA induces BBB development during embryogenesis [35]. Galla's group reported that hydrocortisone enhances the TEER of pig and mouse *in vitro* BBB models and the effect is not species-specific [26, 27]. Hydrocortisone modulates the tight junction formation for cell-cell contact, which is accompanied by modulation of the cytoskeleton and changes in the mechanical properties of the cells [27]. However, in our hiPSC-derived model, hydrocortisone did not enhance the TEER by itself but rather the combination of hydrocortisone and RA significantly induced a higher TEER than each alone. Thus, the combination of hydrocortisone and RA significantly increased the integrity or biophysical barrier properties of this human model. This combination remains to be tested in other models. Furthermore, in the presence of rat primary glial co-culture, the TEER value of our model increased further to 2970 $\Omega.cm^2$ ± 363 $\Omega.cm^2$. The highest TEER value of our *in vitro* model with glial co-culture reached 4185 $\Omega.cm^2$. The glial co-culture thus strongly enhanced the integrity and biophysical barrier property of the *in vitro* BBB monolayer, which is consistent with previous studies indicating an important role of glial cells in BBB properties [14, 28]. It should be emphasized that the use of primary human cells generated from aborted fetuses is a sensitive ethical issue for pharmaceutical companies. Primary fetal human glial cells were thus not tested for co-culture in our model but instead primary rat astroglial cells were used. One functional parameter of BBB integrity is paracellular permeability, which can be determined by LY assay. We found that the TEER value dropped when the culture medium of the *in vitro* BBB model was switched to a transport buffer for drug transport assays. This has also been reported in other studies [15, 28]. During transport assays for small molecules, the TEER values of our *in vitro* model were generally maintained above 1000 $\Omega.cm^2$, and glial co-culture models were used for all the transport assays. The low permeability to LY (<50 nm/s) validated the integrity of the biophysical barrier and low paracellular permeability of the *in vitro* BBB model assays at the functional level, particular with glial co-culture.

One of the most important aspects of *in vitro* BBB models is whether they can mimic the *in vivo* situation and predict the *in vivo* BBB permeability properties of drug candidates. Many of the published *in vitro* BBB models

constituted from primary or iPSC-derived ECs appear to have less predictability for the *in vivo* BBB permeability to CNS drug or have tested few drugs [11, 13–15]. It is thus essential to validate the *in vitro* BBB models with known CNS drug molecules in comparison with the *in vivo* BBB permeability of those drugs. We have demonstrated that our hiPSC-derived BBB model is predictive for the *in vivo* BBB permeability of CNS compounds with passive diffusion properties or are weak Pgp/BCRP substrates by using a correlation analysis formula as described above. Furthermore, the model is also predictive for the *in vivo* BBB permeability of strong Pgp/BCRP substrates by using a different correlation analysis formula. These results demonstrate good biophysical barrier properties and drug transport barrier functionality of the model, respectively. Typically, the first-line screening for new CNS drug candidates is carried out using cell models based on MDCK-MDR1/Pgp and/or MDCK-BCRP. If the compounds are not Pgp/BCRP substrates or weak Pgp/BCRP substrates measured in these cell systems, those compounds are selected for further development, and our iPSC-based human model is useful for testing their BBB permeability and predicting the *in vivo* CNS penetration of those compounds. The CNS permeability of strong Pgp/BCRP substrates can also be evaluated in this model but by using a different correlation analysis formula as described above. Thus, this model will benefit CNS drug development/screening, particularly in industrial settings.

It is known that none of the existing *in vitro* BBB models can perfectly mimic all the features and functions of the *in vivo* BBB or neurovascular unit. As reported in other studies [11], Pgp was also expressed and functional in our model, and the presence of the Pgp inhibitor GF120918 inhibited Pgp-mediated drug efflux and directional pumping. According to published data, glial co-culture induces the polarity of BBB cells and/or increases the expression and function of efflux transporters, such as Pgp and BCRP [11, 36, 37]. However, in our model, the co-culture with rat glial cells did not significantly increase the expression of Pgp/BCRP, but did significantly enhance the TEER and integrity of the model.

In summary, the human iPSC line GM25256 can be differentiated into endothelial cells by using a modified and optimized protocol, which provides scalable and renewable human cells for *in vitro* BBB modeling. Co-culture with primary rat astroglial cells significantly enhances the TEER and biophysical barrier properties of the *in vitro* BBB model. Cryopreservation and recovery of hiPSC-derived ACs allow large-scale study/screening of CNS drugs in the industrial setting. Particularly, this hiPSC-derived *in vitro* BBB model can be applied to rapidly screen CNS drug candidate molecules, and to predict the *in vivo* CNS permeability of both Pgp/BCRP substrates and non-Pgp/BCRP substrates by using two different correlation analysis formulae.

Conflict of interest The authors declare that there is no conflict of interest.

References

1. Goodwin JT, Clark DE. In silico predictions of blood-brain barrier penetration: considerations to "keep in mind". J Pharmacol Exp Ther 2005, 315: 477–483.
2. Cho CF, Wolfe JM, Fadzen CM, Calligaris D, Hornburg K, Chiocca EA, *et al.* Blood-brain-barrier spheroids as an in vitro screening platform for brain-penetrating agents. Nat Commun 2017, 8: 15623.
3. Abbott NJ. Prediction of blood-brain barrier permeation in drug discovery from in vivo, in vitro and in silico models. Drug Discov Today Technol 2004, 1:407–416.
4. Liu HF, Dong K, Zhang W, Summerfield SG, Terstappen GC. Prediction of brain-to-blood unbound concentration ratios in CNS drug discovery employing in silico and in vitro model systems. Drug Discov Today 2018, 23: 1357–1372.
5. Eigenmann DE, Xue G, Kim KS, Moses AV, Hamburger M, Oufir M. Comparative study of four immortalized human brain capillary endothelial cell lines, hCMEC/D3, hBMEC, TY10, and BB19, and optimization of culture conditions, for an in vitro blood-brain barrier model for drug permeability studies. Fluids Barriers CNS 2013, 10: 33.
6. Helms HC, Abbott NJ, Burek M, Cecchelli R, Couraud PO, Deli MA, *et al.* In vitro models of the blood-brain barrier: An overview of commonly used brain endothelial cell culture models and guidelines for their use. J Cereb Blood Flow Metab 2016, 36: 862–890.
7. Weksler BB, Subileau EA, Perrière N, Charneau P, Holloway K, Leveque M, *et al.* Blood-brain barrier-specific properties of a human adult brain endothelial cell line. FASEB J 2005, 19: 1872–1874.
8. Israel MA, Yuan SH, Bardy C, Reyna SM, Mu Y, Herrera C, *et al.* Probing sporadic and familial Alzheimer's disease using induced pluripotent stem cells. Nature. 2012, 482: 216–220.
9. Dolmetsch R, Geschwind DH. The human brain in a dish: the promise of iPSC-derived neurons. Cell 2011, 145: 831–834.
10. Vatine GD, Al-Ahmad A, Barriga BK, Svendsen S, Salim A, Garcia L, *et al.* Modeling Psychomotor retardation using iPSCs from MCT8-deficient patients indicates a prominent role for the blood-brain barrier. Cell Stem Cell 2017, 20: 831–843.e5.
11. Lippmann ES, Al-Ahmad A, Azarin SM, Palecek SP, Shusta EV. A retinoic acid-enhanced, multicellular human blood-brain barrier model derived from stem cell sources. Sci Rep 2014, 4: 4160.
12. Lim RG, Quan C, Reyes-Ortiz AM, Lutz SE, Kedaigle AJ, Gipson TA, *et al.* Huntington's disease iPSC-derived brain microvascular endothelial cells reveal WNT-mediated angiogenic and blood-brain barrier deficits. Cell Rep 2017, 19: 1365–1377.
13. Lippmann ES, Azarin SM, Kay JE, Nessler RA, Wilson HK, Al-Ahmad A, *et al.* Derivation of blood-brain barrier endothelial cells from human pluripotent stem cells. Nat Biotechnol 2012, 30: 783–791.
14. Cecchelli R, Berezowski V, Lundquist S, Culot M, Renftel M, Dehouck MP, *et al.* Modelling of the blood-brain barrier in drug discovery and development. Nat Rev Drug Discov 2007, 6: 650–661.

15. Ribecco-Lutkiewicz M, Sodja C, Haukenfrers J, Haqqani AS, Ly D, *et al.* A novel human induced pluripotent stem cell blood-brain barrier model: Applicability to study antibody-triggered receptor-mediated transcytosis. Sci Rep 2018, 8: 1873.
16. Katt ME, Xu ZS, Gerecht S, Searson PC. Human brain microvascular endothelial cells derived from the BC1 iPS cell line exhibit a blood-brain barrier phenotype. PLoS One 2016, 11: e0152105.
17. Skaper SD, Facci L. Culture of neonatal rodent microglia, astrocytes, and oligodendrocytes from the cortex, spinal cord, and cerebellum. Methods Mol Biol 2018, 1727: 49–61.
18. Triguero D, Buciak J, Pardridge WM. Capillary depletion method for quantification of blood-brain barrier transport of circulating peptides and plasma proteins. J Neurochem 1990, 54: 1882–1888.
19. Rautio J, Humphreys JE, Webster LO, Balakrishnan A, Keogh JP, Kunta JR, *et al.* In vitro P-glycoprotein inhibition assays for assessment of clinical drug interaction potential of new drug candidates: a recommendation for probe substrates. Drug Metab Dispos 2006, 34: 786–792.
20. Liu H, Huang L, Li Y, Fu T, Sun X, Zhang YY, *et al.* Correlation between membrane protein expression levels and transcellular transport activity for breast cancer resistance protein (BCRP). Drug Metabo Dispos 2017, 45: 449–456.
21. Wilson HK, Faubion MG, Hjortness MK, Palecek SP, Shusta EV. Cryopreservation of brain endothelial cells derived from human induced pluripotent stem cells is enhanced by rho-associated coiled coil-containing kinase inhibition. Tissue Eng Part C Methods 2016, 22: 1085–1094.
22. El Hafny B, Bourre JM, Roux F. Synergistic stimulation of γ-glutamyl transpeptidase and alkaline phosphatase activities by retinoic acid and astroglial factors in immortalized rat brain microvessel endothelial cells. J Cell Physiol 1996, 167: 451–460.
23. DeBault LE, Cancilla PA. γ-Glutamyl transpeptidase in isolated brain endothelial cells: induction by glial cells in vitro. Science. 1980, 207: 653–655.
24. Xiong H, Callaghan D, Bai JY, Jones A, Rasquinha I, Smith C, *et al.* ABCG2 is up-regulated in Alzheimer's brain with cerebral amyloid angiopathy and may act as a gatekeeper at the blood-brain barrier for Aβ1-40 peptides. J Neurosci 2009, 29: 5463–5475.
25. Furihata T, Kawamatsu S, Ito R, Saito K, Suzuki S, Kishida S, *et al.* Hydrocortisone enhances the barrier properties of HBMEC/ciβ, a brain microvascular endothelial cell line, through mesenchymal-to-endothelial transition-like effects. Fluids Barriers CNS 2015, 12: 7.
26. Hoheisel D, Nitz T, Franke H, Wegener J, Hakvoort A, Tilling T, *et al.* Hydrocortisone reinforces the blood-brain properties in a serum free cell culture system. Biochem Biophys Res Commun 1998, 247: 312–315.
27. Weidenfeller C, Schrot S, Zozulya A, Galla HJ. Murine brain capillary endothelial cells exhibit improved barrier properties under the influence of hydrocortisone. Brain Res 2005, 1053: 162–174.
28. Mantle JL, Min L, Lee KH. Minimum transendothelial electrical resistance thresholds for the study of small and large molecule drug transport in a human in vitro blood-brain barrier model. Mol Pharm 2016, 13: 4191–4198.
29. Yi X, Liu M, Luo Q, Zhuo H, Cao H, Wang J, *et al.* Toxic effects of dimethyl sulfoxide on red blood cells, platelets, and vascular endothelial cells *in vitro*. FEBS Open Bio 2017, 7:485–494.
30. de Abreu Costa L, Henrique Fernandes Ottoni M, Dos Santos MG, Meireles AB, Gomes de Almeida V, de Fátima Pereira W, *et al.* Dimethyl Sulfoxide (DMSO) decreases cell proliferation and TNF-α, IFN-γ, and IL-2 cytokines production in cultures of peripheral blood lymphocytes. Molecules 2017, 22. pii: E1789.
31. Nakagawa S, Deli MA, Kawaguchi H, Shimizudani T, Shimono T, Kittel A, *et al.* A new blood-brain barrier model using primary rat brain endothelial cells, pericytes and astrocytes. Neurochem Int 2009, 54: 253–263.
32. Summerfield SG, Read K, Begley DJ, Obradovic T, Hidalgo IJ, Coggon S, *et al.* Central nervous system drug disposition: the relationship between in situ brain permeability and brain free fraction. J Pharmacol Exp Ther 2007, 322: 205–213.
33. Liu H, Li Y, Lu S, Wu Y, Sahi J. Temporal expression of transporters and receptors in a rat primary co-culture blood-brain barrier model. Xenobiotica 2014, 44: 941–951.
34. Korjamo T, Heikkinen AT, Mönkkönen J. Analysis of unstirred water layer in in vitro permeability experiments. J Pharm Sci 2009, 98: 4469–4479.
35. Mizee MR, Wooldrik D, Lakeman KA, van het Hof B, Drexhage JA, Geerts D, *et al.* Retinoic acid induces blood-brain barrier development. J Neurosci 2013, 33: 1660–1671.
36. Al Ahmad A, Gassmann M, Ogunshola OO. Maintaining blood-brain barrier integrity: pericytes perform better than astrocytes during prolonged oxygen deprivation. J Cell Physiol 2009, 218: 612–622.
37. Al Ahmad A, Taboada CB, Gassmann M, Ogunshola OO. Astrocytes and pericytes differentially modulate blood-brain barrier characteristics during development and hypoxic insult. J Cereb Blood Flow Metab 2011, 31: 693–705.
38. Kikuchi R, de Morais SM, Kalvass JC, In vitro P-glycoprotein efflux ratio can predict the in vivo brain penetration regardless of biopharmaceutics drug disposition classification system class. Drug Metab Dispos 2013. 41: 2012–2017.
39. Summerfield SG, Zhang Y, Liu H, Examining the uptake of central nervous system drugs and candidates across the blood-brain barrier. J Pharmacol Exp Ther 2016. 358: 294–305.